Neurobiology of Disease 129 (2019) 44–55

Contents lists available at ScienceDirect

Neurobiology of Disease

journal homepage: www.elsevier.com/locate/ynbdi

Neonatal treatment with cyclosporine A restores neurogenesis and spinogenesis in the Ts65Dn model of Down syndrome

Fiorenza Stagni[a,1], Maria Elisa Salvalai[b,1], Andrea Giacomini[a], Marco Emili[a], Beatrice Uguagliati[a], Er Xia[b], Mariagrazia Grilli[b], Renata Bartesaghi[a,*], Sandra Guidi[a,*]

[a] Department of Biomedical and Neuromotor Sciences, University of Bologna, Bologna, Italy
[b] Department of Pharmaceutical Sciences, University of Piemonte Orientale, Italy

ARTICLE INFO

Keywords:
Down syndrome
Neurogenesis
Spinogenesis
Pharmacotherapy
Cyclosporine A

ABSTRACT

Down syndrome (DS), a genetic condition due to triplication of chromosome 21, is characterized by reduced proliferation of neural progenitor cells (NPCs) starting from early life stages. This defect is worsened by a reduction of neuronogenesis (accompanied by an increase in astrogliogenesis) and dendritic spine atrophy. Since this triad of defects underlies intellectual disability, it seems important to establish whether it is possible to pharmacologically correct these alterations. In this study, we exploited the Ts65Dn mouse model of DS in order to obtain an answer to this question. In the framework of an *in vitro* drug-screening campaign of FDA/EMA-approved drugs, we found that the immunosuppressant cyclosporine A (CSA) restored proliferation, acquisition of a neuronal phenotype, and maturation of neural progenitor cells (NPCs) from the subventricular zone (SVZ) of the lateral ventricle of Ts65Dn mice. Based on these findings, we treated Ts65Dn mice with CSA in the postnatal period P3-P15. We found that treatment fully restored NPC proliferation in the SVZ and in the subgranular zone of the hippocampal dentate gyrus, and total number of hippocampal granule cells. Moreover, CSA enhanced development of dendritic spines on the dendritic arbor of the granule cells whose density even surpassed that of euploid mice. In hippocampal homogenates from Ts65Dn mice, we found that CSA normalized the excessive levels of p21, a key determinant of proliferation impairment. Results show that neonatal treatment with CSA restores the whole triad of defects of the trisomic brain. In DS CSA treatment may pose caveats because it is an immunosuppressant that may cause adverse effects. However, CSA analogues that mimic its effect without eliciting immunosuppression may represent practicable tools for ameliorating brain development in individuals with DS.

1. Introduction

Intellectual disability is one of the most serious problems in Down syndrome (DS), a genetic condition caused by triplication of chromosome 21. The impairment of brain function, which is already detectable in infants with DS, is attributable to severe impairment of key neurodevelopmental processes. In particular, evidence in fetuses/infants with DS and in DS mouse models shows that trisomic neural precursor cells have a reduced proliferation rate and exhibit an altered differentiation program that causes a reduction in the number of cells that differentiate into neurons and an increase in the number of cells that differentiate into astrocytes (Dierssen, 2012; Stagni et al., 2018). Neuronal maturation is also altered in DS, which leads to neurons with a reduced dendritic arborization and a reduced density of dendritic spines. The unavoidable outcome of these defects is the impairment of overall brain wiring, explaining the alteration within a constellation of cognitive domains that characterizes DS.

Intense efforts are currently underway in order to establish whether it is possible to pharmacologically ameliorate intellectual disability in DS. In this connection, there are two possible and not mutually exclusive approaches. One possibility is to use drugs that specifically target cellular pathways that are altered in the DS brain and that are known to regulate one or more of the neurodevelopmental processes mentioned above. This approach requires preliminary knowledge regarding the molecular alterations of the DS brain, the choice of the molecular pathway to be targeted, and the choice of the drug that putatively acts on this pathway. A second possibility is the repositioning of drugs/compounds that were designed and approved for other

* Corresponding authors at: Department of Biomedical and Neuromotor Sciences, Physiology Building, Piazza di Porta San Donato 2, I-40126 Bologna Bo, Italy.
E-mail addresses: renata.bartesaghi@unibo.it (R. Bartesaghi), sandra.guidi3@unibo.it (S. Guidi).
[1] These authors contributed equally to this work.

https://doi.org/10.1016/j.nbd.2019.05.005
Received 20 July 2018; Received in revised form 21 November 2018; Accepted 10 May 2019
Available online 11 May 2019
0969-9961/

pathologies. Various studies show that drugs designed for quite different purposes may actually exert some benefits in various brain disorders. Thus, this strategy is not simply based on an *a priori* assumption. This approach requires i) the development of a reproducible and sensitive phenotypic assay, based on relevant defective properties of trisomic neural progenitor cells (NPCs); ii) a subsequent *in vitro* screening of libraries of clinically approved drugs in the search for those that may revert that phenotype. In principle, cell-based screening combined with strategies of drug repurposing offers the opportunity to significantly reduce risks and costs associated with developing new therapeutics and, more importantly, may dramatically reduce time for human translation. By following this strategy, we aim to identify clinically approved drugs that are able to restore proliferative and differentiative defects of NPCs derived from the Ts65Dn mouse, a widely-used model of DS. After *in vitro* identification of effective molecules, our final goal is to test their effects *in vivo* in the Ts65Dn mouse. Herein we show the identification of the immunosuppressant and clinically relevant cyclosporine A (CSA) as a drug that can not only restore the proliferation rate of NPCs and their differentiation into neurons *in vitro*, but that is also effective *in vivo* in the Ts65Dn mouse. According to recent work, a dose of 15.0 mg/kg/day of CSA increases the pool of actively dividing cells in the dentate gyrus of wild type mice and also favors the generation of new granule neurons (Chow and Morshead, 2016). We show here that neonatal treatment with 15.0 mg/kg/day of CSA for a short period of time (13 days) restores proliferation of NPCs in the two major brain neurogenic niches (the subventricular zone and the subgranular zone of the hippocampal dentate gyrus) of Ts65Dn mice and reinstates hippocampal development, in terms of granule cell number and spinogenesis. This provides evidence that treatment with a single drug can rescue the major neurodevelopmental defects of the DS brain.

2. Methods

2.1. Colony

Ts65Dn mice were generated by mating B6EiC3Sn a/A-Ts(17ˆ16)65Dn females with C57BL/6JEiJ x C3H/HeSnJ (B6EiC3Sn) F1 hybrid males. This parental generation was provided by Jackson Laboratories (Bar Harbor, ME, USA). To maintain the original genetic background, the mice used were of the first generation of this breeding. Animals were genotyped as previously described (Reinholdt et al., 2011). The day of birth was designated postnatal day zero (P0). The animals' health and comfort were controlled by the veterinary service. The animals had access to water and food *ad libitum* and lived in a room with a 12:12 h light/dark cycle. Experiments were performed in accordance with the European Communities Council Directive of 24 November 1986 (86/609/EEC) for the use of experimental animals and were approved by Italian Ministry of Public Health. In this study, all efforts were made to minimize animal suffering and to keep the number of animals used to a minimum.

3. *In vitro* experiments

3.1. Isolation and culture of SVZ neural progenitor cells

Cells were isolated from the subventricular zone (SVZ) of the lateral ventricle of newborn (age 1–2 days) euploid and Ts65Dn mice, as previously described (Stagni et al., 2017). Briefly, brains were removed, the SVZ region was isolated and collected in ice-cold PIPES buffer pH 7.4. After centrifugation, tissue was digested for 10 min at 37 °C using Trypsin/EDTA 0.25% (Life Technologies) aided by gentle mechanical dissociation. Cell suspensions from individual mice were pooled and plated onto 25 cm^2 cell-culture flask (Thermo Fisher Scientific) and cultured as floating neurospheres in medium containing basic fibroblast growth factor (bFGF, 10 ng/ml; Peprotech) and epidermal growth factor (EGF, 20 ng/ml; Peprotech) using an established protocol (Meneghini et al., 2014). Primary (Passage 1, P1) neurospheres were dissociated using Stempro Accutase (Life Technologies) after 7 days *in vitro* (DIV); thereafter neurospheres were passaged every 5 DIV. For further *in vitro* studies cells from P3 to P12 were used.

3.2. Phenotypic drug screening

For the drug screening, two different commercial libraries (Prestwick chemical library®, Prestwick Chemical, and Screen-Well® FDA Approved Drug Library V2, Enzo Life Sciences), containing a total of 1887 FDA/EMA-approved drugs were used. These libraries were chosen for their chemical and pharmacological diversity. Trisomic SVZ NPCs (P3-P12) pooled from at least 3–5 pups were dissociated in a single cell suspension and plated onto Nunclon™ Delta Surface 96-well plate (Thermo Fisher Scientific) at a density of 4×10^3 cells per well in DMEM/F-12 medium supplemented with B27, Glutamax™ (2 mM, Life Technologies), heparin sodium salt (4 μg/ml; ACROS Organics), bFGF (10 ng/ml, Peprotech) and 100 U/100 μg/ml Penicillin/Streptomycin (Life Technologies) for 30 min, at 37 °C. Compounds were added to each well in quadruplicates (1 μM final concentration, in 0.05% DMSO). In parallel, EGF (20 ng/ml, Peprotech) and LiCl (2 mM, Sigma-Aldrich), that have been shown to restore proliferation of NPCs of Ts65Dn mice *in vivo* (Bianchi et al., 2010a; Contestabile et al., 2013) and *in vitro* (Trazzi et al., 2014), were added to each plate in quadruplicates as pro-proliferative controls. Lithium concentration was chosen based on previous evidence (Trazzi et al., 2014). Cell proliferation was quantified after 96 h incubation in a humidity chamber (to minimize evaporation) and quantified as relative luminescence units (RLU) values using a CellTiter-Glo ATP-based assay kit (Promega) on a Victor^3-V plate reader (PerkinElmer) (Stagni et al., 2017). Drug activity was calculated as percentage of change compared to basal conditions (cells grown in presence of 10 ng/ml FGF and 0.05% DMSO). The same proliferation assay was performed to assess hit concentration response curves (0.1–1000 nM).

3.3. Neural progenitor cell proliferation and differentiation

In order to evaluate cell proliferation in secondary assays, EdU (5-ethynyl-2-deoxyuridine) incorporation was performed using the Click-iT® EdU Alexa Fluor® 488 HCS Assay Kit (Thermo Fisher Scientific). Briefly, neurospheres (P3-P12) were dissociated in a single cell suspension and plated onto laminin-coated 96-well plate (Falcon) at a density of 4×10^3 cells per well in DMEM/F-12 medium supplemented with B27, Glutamax™, heparin sodium salt (4 μg/ml; ACROS Organics), bFGF (10 ng/ml) and 100 U/100 μg/ml Penicillin/Streptomycin (Life Technologies) in presence of CSA (1000 nM; MedChem Express) or its vehicle (DMSO 0.05%) for 72 h. In the last 12 h period, EdU was added to each well at a final concentration of 10 μM. After that, cells were fixed for 20 min at room temperature using 4% paraformaldehyde in phosphate-buffered saline (PBS, pH 7.4). EdU detection was performed according to manufacturer's instructions. In each experiment, 37 fields/well (corresponding to about 50% of the total well surface) were counted using an InCell Analyzer 2200 (GE). Cell death was evaluated using the CytoTox-Glo™ Cytotoxicity Assay (Promega) according to the manufacturer's instructions. Cells were exposed to CSA (30–1000 nM, MedChem Express) or its vehicle (DMSO 0.05%) for 96 h. Cytotoxicity was quantified as relative luminescence unit (RLU) on a Victor^3-V plate reader (PerkinElmer) and expressed as percentage over the total number of cells. For differentiation experiments neurospheres from the SVZ were dissociated into single cells and plated onto laminin-coated Lab-Tek 8-well permanox chamber slides (Thermo Fisher Scientific) at a density of 35×10^3 per well in differentiation medium (DMEM-F12 supplemented with B27, 2 mM Glutamax and 100 U/100 mg/ml penicillin/streptomycin). NPCs were treated in presence of CSA (3–1000 nM) or vehicle (DMSO 0.05%) for 96 h. After that, cells were fixed for 20 min at room temperature using 4% paraformaldehyde. Phenotypic characterization of NPC-derived cells was carried out by

immunolocalization for MAP2 (rabbit polyclonal, 1:50000; Abcam) and Nestin (chicken monoclonal, 1:2500; Neuromics). Secondary antibodies were as follows: AlexaFluor555-conjugated goat anti rabbit (1:1400; MolecularProbes), and AlexaFluor488-conjugated goat anti chicken (1:1400; Molecular Probes). In additional experiments, in which trisomic and euploid NPCs were exposed to selected concentrations of CSA (100–1000 nM) or vehicle for 96 h, we evaluated, in parallel to MAP2/nestin, GFAP immunoreactivity using a mouse anti-GFAP monoclonal antibody (1:600, Millipore), and a secondary AlexaFluor555-conjugated goat anti mouse antibody (1:1600; Molecular Probes). Nuclei were counterstained with 0.8 ng/ml Hoechst (Thermo Fisher Scientific) diluted in PBS. In each experiment, five fields/well (corresponding to about 150–200 cells/well) were counted with a 60× objective by a Leica DMIRB inverted fluorescence microscope. Immunoreactive cells were counted and their percentage over total viable cells was calculated. In differentiating cultures exposed to CSA (3–1000 nM) for 96 h, the number of $MAP2^+$ cells exhibiting neuritic processes was counted at random locations in three fields/well and their number was expressed as the percentage over total cell number in each sampled location. All experiments were run in triplicate.

4. *In vivo* experiments

4.1. Experimental protocol

According to recent work, a dose of 15.0 mg/kg/day of CSA has a pro-neurogenic effect in the dentate gyrus of adult wild type mice (Chow and Morshead, 2016). Based on this evidence, we treated euploid and Ts65Dn mice with CSA (MedChem Express, 15.0 mg/kg/day in vehicle; s.c. injection) or vehicle (PBS with 2.5% DMSO) from postnatal day 3 (P3) to P15. Mice that received CSA will hereafter be called "treated mice" (treated euploid mice: $n = 15$; treated Ts65Dn mice: $n = 14$). Mice that received the vehicle will be called "untreated mice" (untreated euploid mice: $n = 21$; untreated Ts65Dn mice: n = 21). Each experimental group was composed of a similar number of males and females (treated euploid mice: 8 males, 7 females; treated Ts65Dn mice: 8 males, 6 females; untreated euploid mice: 10 males, 11 females; untreated Ts65Dn mice: 11 males, 10 females). On P15, mice received a subcutaneous injection (150 µg/g body weight) of BrdU in TrisHCl 50 mM 2 h before being killed. The brains were excised and cut along the midline. The left hemispheres of a group of mice were fixed by immersion in PFA 4% and frozen, and the right hemispheres were used for Golgi staining. The right hemispheres of other mice were kept at −80 °C and used for western blotting. The body weight of mice of all groups was recorded prior to sacrifice and the brain weight was recorded immediately after brain removal. The number of animals used for each experimental procedure is specified in the figure legends. In order to establish whether lower doses of CSA have a pro-neurogenic effect in Ts65Dn mice similar to that elicited by the 15.0 mg/kg dose (see Results), we also tested the effects of 1.5 mg/kg ($n = 6$ mice: 3 males, 3 females) or 7.5 mg/kg ($n = 4$ mice: 3 males, 1 female) of CSA (same protocol as above).

4.2. Histological procedures

The frozen brains were cut with a freezing microtome into 30-µm-thick coronal sections that were serially collected in anti-freezing solution (30% glycerol; 30% ethylen-glycol; 10% PBS 10×; sodium azide 0.02%; MilliQ to volume).

4.2.1. Hoechst-staining

One out of six free-floating sections taken from the beginning to the end of the hippocampal formation ($n = 15$–19 sections) were incubated for 2 min in Hoechst nuclear dye (2 mg/ml in PBS) and mounted on slides.

4.2.2. BrdU immunohistochemistry

Immunohistochemistry was carried out as previously described (Contestabile et al., 2007; Bianchi et al., 2010b; Guidi et al., 2013; Giacomini et al., 2015). One out of six free-floating sections (n = 15–19 sections) from the hippocampal formation was incubated with rat anti-BrdU antibody (diluted 1:200; Biorad) and detection was performed with a Cy3-conjugated anti rat-secondary antibody (diluted 1:200; Jackson Immunoresearch). Sections were then mounted on slides.

4.2.3. Golgi staining

Brains were Golgi stained using the FD Rapid Golgi Stain ™ Kit (FD Neuro Technologies, Inc.). Brains were immersed in the impregnation solution containing mercuric chloride, potassium dichromate and potassium chromate (the impregnation solution was prepared by mixing equal volumes of Solutions A and B of the FD Rapid Golgi Stain ™ Kit) and stored at room temperature in the dark for 2 weeks. Then, brains were transferred into Solution C (FD Rapid Golgi Stain ™ Kit) and stored at room temperature in the dark for at least 72 h. After these steps, hemispheres were cut with a microtome into 90-µm-thick coronal sections that were mounted on gelatin-coated slides, and were air dried at room temperature in the dark for at least one day. After drying, sections were rinsed with distilled water and subsequently stained in a developing solution (FD Rapid Golgi Stain Kit).

4.3. Image acquisition

Immunofluorescence images were taken with a Nikon Eclipse TE 2000-S inverted microscope (Nikon Corp., Kawasaki, Japan), equipped with a Nikon digital camera DS-Qi2. Bright field images were taken on a light microscope (Leitz) equipped with a motorized stage and focus control system and a Coolsnap-Pro color digital camera (Media Cybernetics, Silver Spring, MD, USA). Measurements were carried out using the software Image Pro Plus (Media Cybernetics, Silver Spring, MD 20910, USA).

4.4. Measurements

4.4.1. Number of BrdU-positive cells

BrdU-positive cells in the dentate gyrus and the region of the SVZ that spans along the whole rostro-caudal extent of the hippocampal formation were detected using a fluorescence microscope (Eclipse; objective: 20x, 0.5 NA). Quantification of BrdU-labeled nuclei was conducted in every 6th section using a modified unbiased stereology protocol that has previously been reported to successfully quantify BrdU labeling (Malberg et al., 2000; Kempermann and Gage, 2002; Tozuka et al., 2005). All BrdU-labeled cells located in the granule cell layer and subgranular zone and in the SVZ were counted in their entire z axis (1 µm steps) in each section. To avoid oversampling errors, nuclei intersecting the uppermost focal plane were excluded. The total number of BrdU-labeled cells per animal was determined and multiplied by six to obtain the total estimated number of cells per dentate gyrus and per SVZ.

4.4.2. Stereology of the dentate gyrus

Unbiased stereology was performed on Hoechst-stained sections. The optical disector method was used to obtain density, and the Cavalieri principle was used to estimate volume, as previously described (Stagni et al., 2017).

Spine density. In Golgi-stained sections from the dentate gyrus, spines of granule cells were counted using a 100× oil immersion objective lens (1.4 NA). Spine density values were evaluated in dendritic segments located in the inner (proximal dendrites) and outer (distal dendrites) half of the molecular layer. For each neuron, 3–4 proximal and 3–4 distal segments were analyzed. For each animal, spines were counted in at least 4 neurons. The length of each sampled dendritic segment was determined by tracing its profile and the number of spines

was counted manually. The linear spine density was calculated by dividing the total number of spines by the length of the dendritic segment. Spine density was expressed as number of spines per 100 μm dendrite.

4.5. Western blotting

In homogenates of the hippocampal formation, total proteins were obtained as previously described (Trazzi et al., 2011) and the levels of p21 (1:200, Santa Cruz Biotechnology; catalog number: sc-271532) were evaluated. Densitometric analysis of digitized images with ChemiDoc XRS+ was performed with Image Lab software (Bio-Rad Laboratories, Hercules, CA, USA) and intensity for each band was normalized to the intensity of the Ponceau S staining. This evaluation has the advantage that it does not rely on a single protein for normalization, thereby circumventing the possibility that the chosen "housekeeping" proteins may vary in some conditions (Romero-Calvo et al., 2010).

4.6. Statistical analysis

Results are presented as mean ± standard error of the mean (SE). Data were analyzed with the IBM SPSS 22.0 software. Before running statistical analyses, we checked data distribution and homogeneity of variances for each variable using the Shapiro-Wilk test and Levene's test respectively. Data were normally distributed with the exception of granule cell density. In this case, statistical analysis was carried out using the Kruskal-Wallis test followed by the Mann–Whitney *U* test. For all other examined variables statistical analysis was carried out using either a one-way ANOVA or a two-way ANOVA with genotype (euploid, Ts65Dn) and treatment (vehicle, CSA), as factors. *Post hoc* multiple comparisons were carried out using Fisher's least significant difference (LSD) test. Based on the "Box plot" tool available in SPSS Descriptive Statistics, in each analysis we excluded the extremes, *i.e.*, values that were larger than 3 times the IQ range [x ≥ Q3 + 3 * (IQ); x ≤ Q1–3 * (IQ)]. The number of mice included in (and excluded from, if any) individual analyses is reported in the legends of figures and Table 1. A probability level of $p \leq .05$ was considered to be statistically significant.

5. Results

5.1. Identification and characterization of CSA effects in trisomic NPC phenotypic assays

NPCs from the SVZ of neonate Ts65Dn mice exhibit impairment of proliferation rate, similarly to the *in vivo* condition (Trazzi et al., 2011; Trazzi et al., 2013; Stagni et al., 2017). As result of a screening effort, among 1887 tested FDA-EMA drugs the immunosuppressant CSA was identified as a drug promoting proliferation of trisomic NPCs (% increase of proliferation: +53% at 1000 nM *vs.* basal conditions) [$F(2,15) = 56.10$, $p < .001$] (Fig. 1A). We used as a positive control lithium chloride, a well-established *in vivo* neurogenesis enhancer in DS (Bianchi et al., 2010a; Contestabile et al., 2013; Trazzi et al., 2014; Stagni et al., 2017), and found that lithium chloride at 2 mM enhanced proliferation by +39% *vs.* basal conditions [$F(2,15) = 56.10$, $p < .001$] (Fig. 1A).

CSA was then tested under a wide range of concentrations (0.1–1000 nM). A one-way ANOVA showed a significant effect of treatment [$F(5,42) = 10.855$, $p < .001$]. A *post hoc* Fisher's LSD test showed that CSA concentrations of 0.1–100 nM had no significant effect on proliferation, while a concentration of 1000 nM increased the number of trisomic NPCs (Fig. 1B). By using a cytotoxicity assay, we could exclude that CSA-mediated effect on the number of NPCs was due to increased cell viability. Indeed, none of the tested CSA concentrations affected cell death rate (Fig. 1C). In order to obtain more direct evidence on the pro-proliferative effect of CSA, we evaluated the proliferation rate based on incorporation of the thymidine analogue EdU (5-ethynyl-2-deoxyuridine) in trisomic and euploid cultures exposed to CSA (1000 nM) or vehicle. A two-way ANOVA showed a genotype x treatment interaction [$F(1,8) = 72.531$, $p < .001$], a main effect of genotype [$F(1,8) = 277.386$, $p < .001$] and a main treatment [$F(1,8) = 262.037$, $p < .001$]. A *post hoc* Fisher's LSD test showed that trisomic and euploid cells exposed to CSA 1000 nM underwent a proliferation increase in comparison with their untreated counterparts (Fig. 1D). Importantly, in response to CSA treatment, trisomic NPCs displayed a proliferation rate similar to untreated euploid NPCs.

In addition to proliferation impairment, trisomic NPCs exhibit impairment in the acquisition of a neuronal phenotype and in neuronal maturation, *i.e.*, development of neuritic processes (Trazzi et al., 2011; Trazzi et al., 2013; Stagni et al., 2017). In cultures of NPCs under differentiating conditions we evaluated the percentage of cells that were i) immunopositive to MAP2 (a marker of cells with a neuronal phenotype) and immunonegative to Nestin (a marker of undifferentiated NPCs); ii) double immunopositive to MAP2 and Nestin, *i.e.*, neuroblasts; iii) immunonegative to MAP2 and to Nestin (putative glial cells). A one-way ANOVA on the percentage of cells that were MAP2-positive and Nestin-negative ($MAP2^+/Nestin^-$) showed a significant effect of treatment [$F(6,14) = 7.735$, $p < .001$]. Fisher's LSD test, carried out *post hoc*, showed that drug concentrations of 100–1000 nM caused a significant increase in the percentage of $MAP2^+/Nestin^-$ cells in comparison with cultures treated with vehicle (Fig. 1E), suggesting that CSA favors the acquisition of a neuronal phenotype. A one-way ANOVA on the percentage of cells that were MAP2-positive and Nestin-positive ($MAP2^+/Nestin^+$) showed no effect of treatment [$F(6,14) = 2.182$, $p < .108$] (Fig. 1F) suggesting that treatment does not affect the population of neuroblasts. An evaluation of the percentage of cells that were negative to both MAP2 and Nestin ($MAP2^-/Nestin^-$) showed a significant effect of treatment [$F(6,14) = 5.389$, $p < .004$]. A *post hoc* Fisher's LSD test

Table 1
Effect of treatment with CSA on body and brain weight

		n.	Mean		SE		n.	Mean		SE	*p*
Body	Euploid + Veh	21	7.58	±	0.20	Euploid + CSA	15	8.72	±	0.38	0.015
	Ts65Dn + Veh	21	6.65	±	0.37	Ts65Dn + CSA	14	6.09	±	0.38	0.228
	p		0.031					0.001			
Brain	Euploid + Veh	20	0.40	±	0.01	Euploid + CSA	14	0.39	±	0.01	0.054
	Ts65Dn + Veh	20	0.39	±	0.01	Ts65Dn + CSA	14	0.37	±	0.01	0.049
	p		0.005					0.016			

Body weight and brain weight (mean ± SE), in grams, of euploid and Ts65Dn mice that received either vehicle (Veh) or cyclosporine A (CSA; 15.0 mg/kg) in the period P3-P15, measured on P15. The *p* value in the row below each variable refers to the comparison between untreated euploid (Euploid + Veh) and Ts65Dn (Ts65Dn + Veh) mice, and treated euploid (Euploid + CSA) and Ts65Dn (Ts65Dn + CSA) mice. The column "n." reports the number of animals included in the statistical analysis. For the brain weight analysis, we excluded one untreated euploid mouse, one untreated Ts65Dn mouse, and one treated euploid mouse, based on the criteria explained in the Statistics section. The *p* value in the column on the right refers to the comparison between untreated and treated mice of the same genotype (Fisher's LSD test after two-way ANOVA).

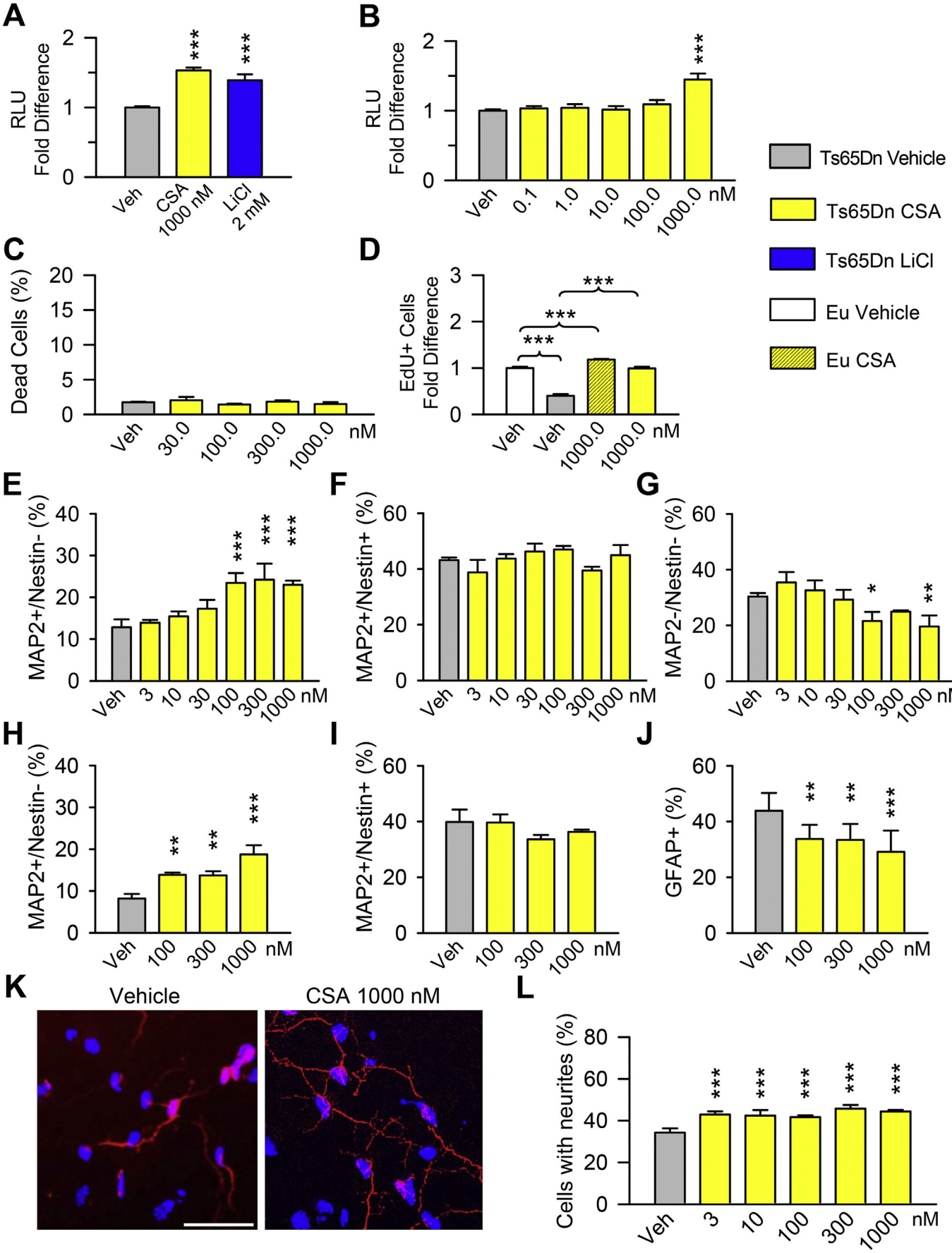

(caption on next page)

Fig. 1. Effect of CSA on proliferation, differentiation and maturation of NPCs derived from the SVZ.
A,B: Effect of CSA 1000 nM or LiCl 2.0 mM (A) and of different concentrations of CSA (B) on the proliferation rate (evaluated as relative luminescence units, RLU; see Methods) of NPCs of Ts65Dn mice at 96 h in culture. Data are expressed as fold change in comparison with NPCs exposed to vehicle alone (DMSO 0.05%). C: Percentage of dead cells in trisomic cultures exposed to different concentrations of CSA for 96 h. D: EdU-positive cells in cultures of euploid and trisomic NPCs exposed to vehicle or to CSA 1000 nM for 72 h. Data are expressed as fold change in comparison with euploid NPCs exposed to vehicle alone. *E-J*: Percentage of $MAP2^+/Nestin^-$ cells (E,H), $MAP2^+/Nestin^+$ cells (F,I), $MAP2^-/Nestin^-$ cells (G), and $GFAP^+$ cells (J) in cultures of trisomic NPCs under differentiating conditions and exposed to the indicated concentrations of CSA for 96 h. K,L: Representative confocal microscope image (K) and percentage (L) of $MAP2^+$ cells (red) exhibiting neuritic processes in cultures of NPCs from the SVZ of Ts65Dn mice grown under differentiating conditions and exposed to the indicated concentrations of CSA for 96 h. Images in (K) show $MAP2^+$ cells that were exposed to either vehicle (DMSO 0.05%) or CSA 1000 nM. Nuclei were counterstained with Hoechst (blue). Scale bar = 50 μm. Data derive from pooled (3–5) mice. The asterisks in A, B, E, G, H, J, and L indicate a difference in comparison with vehicle-treated cultures: * $p \leq .05$; ** $p \leq .01$; *** $p \leq .001$ (Fisher's LSD test after ANOVA). Abbreviations: CSA, cyclosporine A; EdU, 5-ethynyl-2-deoxyuridine; Eu, euploid; GFAP, glial fibrillary acidic protein; LiCl, Lithium chloride; MAP2, microtubule associated protein 2; Veh, vehicle. (For interpretation of the references to color in this figure legend, the reader is referred to the web version of this article.)

showed that concentrations of 100–1000 nM caused a reduction in the percentage of $MAP2^-/Nestin^-$ cells (Fig. 1G). Since cells that are immunonegative to both MAP2 and Nestin mainly represent cells committed to glia (Cvijetic et al., 2017), these results suggest that CSA treatment promotes neuronal differentiation of trisomic NPCs and that this effect takes place at the expense of their commitment toward non-neuronal lineages (glia).

In order to obtain a more direct evidence of the glial nature of $MAP2^-/Nestin^-$ cells, we carried out additional experiments in which we evaluated, in parallel to the percentage of cells that were $MAP2^+/Nestin^-$ or $MAP2^+/Nestin^+$, the percentage of cells expressing the astrocytic marker GFAP. A one-way ANOVA on the percentage of $MAP2^+/Nestin^-$ cells confirmed a significant effect of drug treatment [$F(3,11) = 14.94$, $p = .001$]. Fisher's LSD test, carried out *post hoc*, confirmed that CSA 100–1000 nM caused a significant increase in the percentage of $MAP2^+/Nestin^-$ cells in comparison with vehicle-treated trisomic cells (Fig. 1H). A one-way ANOVA on the percentage of $MAP2^+/Nestin^+$ cells showed again no effect of treatment (Fig. 1I). An evaluation of the percentage of $GFAP^+$ cells showed a significant effect of treatment [$F(3,23) = 8.860$, $p = .001$]. A *post hoc* Fisher's LSD test showed that CSA concentrations 100–1000 nM reduced the percentage of $GFAP^+$ (Fig. 1J). These results confirm our hypothesis that CSA promotes neuronal differentiation of trisomic NPCs at the expense of their commitment toward an astrocytic phenotype. A similar effect was also observed in euploid cultures (Supplementary Fig. 1).

In order to establish the effect of CSA on neuron maturation we evaluated the percentage of cells exhibiting neuritic processes in differentiating cultures of trisomic NPCs exposed to different concentrations of CSA. A one-way ANOVA on the percentage of NPCs that exhibited neuritic processes showed a significant effect of treatment [$F(5,12) = 8.025$, $p = .002$]. Fisher's LSD test, carried out *post hoc*, showed that all tested drug concentrations increased the percentage of cells with neuritic processes in comparison with cultures in presence of vehicle (Fig. 1L). Taken together these data show that CSA increases the proliferation rate and fosters the process of neurogenesis and neuron maturation of trisomic NPCs.

5.2. Effect of neonatal treatment with CSA on neural precursor proliferation in the dentate gyrus and SVZ and of Ts65Dn mice

The early postnatal period is a critical time window for neurogenesis in the SGZ of the hippocampal dentate gyrus. In addition, in neonate mice a prominent proliferation rate is present in the SVZ of the lateral ventricle. This is a neurogenic niche that gives origin to the neurons of the forebrain, prenatally, and thereafter produces granule cells destined to the olfactory bulb, glial cells and, possibly, generates neurons destined to the neocortex (Brazel et al., 2003). In view of the relevance of these two neurogenic niches, in the current study we examined the impact of CSA on the proliferation rate of NPCs both in the dentate gyrus and SVZ of euploid and Ts65Dn mice. To this purpose, we treated mice with 15 mg/kg/day of CSA, because this dose has a pro-neurogenic effect in the dentate gyrus of adult wild type mice (Chow and Morshead, 2016).

A two-way ANOVA on the total number of BrdU-positive cells in the dentate gyrus showed a genotype x treatment interaction [$F(1,16) = 8.995$, $p = .008$], but no main effect of either genotype or treatment. A *post hoc* Fisher's LSD test showed that, in agreement with previous evidence (Bianchi et al., 2010b; Giacomini et al., 2015; Stagni et al., 2016; Stagni et al., 2017), untreated Ts65Dn mice had notably fewer proliferating cells in comparison with untreated euploid mice. The number of proliferating cells in treated Ts65Dn mice underwent a large increase (+26%) and became similar to that of untreated euploid mice (Fig. 2A,B). Treatment had no effect on the number of NPCs in the dentate gyrus of euploid mice (Fig. 2A,B). In order to establish whether doses of CSA lower than 15 mg/kg positively affect cell proliferation, we treated Ts65Dn pups with 1.5 mg/kg or 7.5 mg/kg of CSA in the period P3-P15 and examined the effects of treatment in the dentate gyrus. A one-way ANOVA on the number of BrdU-positive cells in the dentate gyrus of Ts65Dn mice that had received vehicle or 1.5 mg/kg, 7.5 mg/kg, and 15.0 mg/kg of CSA showed a significant effect of treatment [$F(3,17) = 6.374$, $p = .004$]. *Post hoc* LSD test showed that, unlike the dose of 15.0 mg/kg, the doses of 1.5 mg/kg and 7.5 mg/kg did not increase the number of BrdU-positive cells (Fig. 2C).

A two-way ANOVA on the total number of BrdU-positive cells in the SVZ showed no genotype x treatment interaction, whereas a main effect of genotype [$F(1,16) = 21.764$, $p < .001$] and a main effect of treatment [$F(1,16) = 38.978$, $p < .001$] appeared. A *post hoc* Fisher's LSD test showed that Ts65Dn mice had fewer cells in comparison with untreated euploid mice. After treatment with CSA, Ts65Dn mice underwent an increase in the number of proliferating cells (+25%) that became similar to that of untreated euploid mice (Fig. 3B). In the SVZ of euploid mice, treatment caused an increase in the number of proliferating cells that became larger (+21%) in comparison with that of their untreated counterparts (Fig. 3B).

These results show that neonatal treatment with CSA is able to restore the proliferation rate of NPCs in both the dentate gyrus and SVZ of Ts65Dn mice.

5.3. Effect of CSA on the stereology of the dentate gyrus of Ts65Dn mice

In the hippocampal dentate gyrus the production of granule cells mainly takes place in the first two postnatal weeks (Altman and Bayer, 1975). Thus, in view of the treatment-induced increase in the proliferation potency of NPCs of the SGZ, we expected this effect to lead to improvement/restoration of the defective cellularity that characterizes the dentate gyrus of trisomic mice. To clarify this issue, we stereologically evaluated the total number of granule cells in treated and untreated mice. A two-way ANOVA on the volume of the dentate gyrus showed no genotype x treatment interaction, but a main effect of genotype [$F(1,15) = 8.705$, $p = .010$], and of treatment [$F(1,15) = 8.887$, $p = .009$]. Fisher's LSD test, carried out *post hoc*, showed that the volume of the granule cell layer of untreated Ts65Dn mice was reduced (Fig. 4B) in comparison with that of euploid mice and that treatment restored the volume of the granule cell layer. The

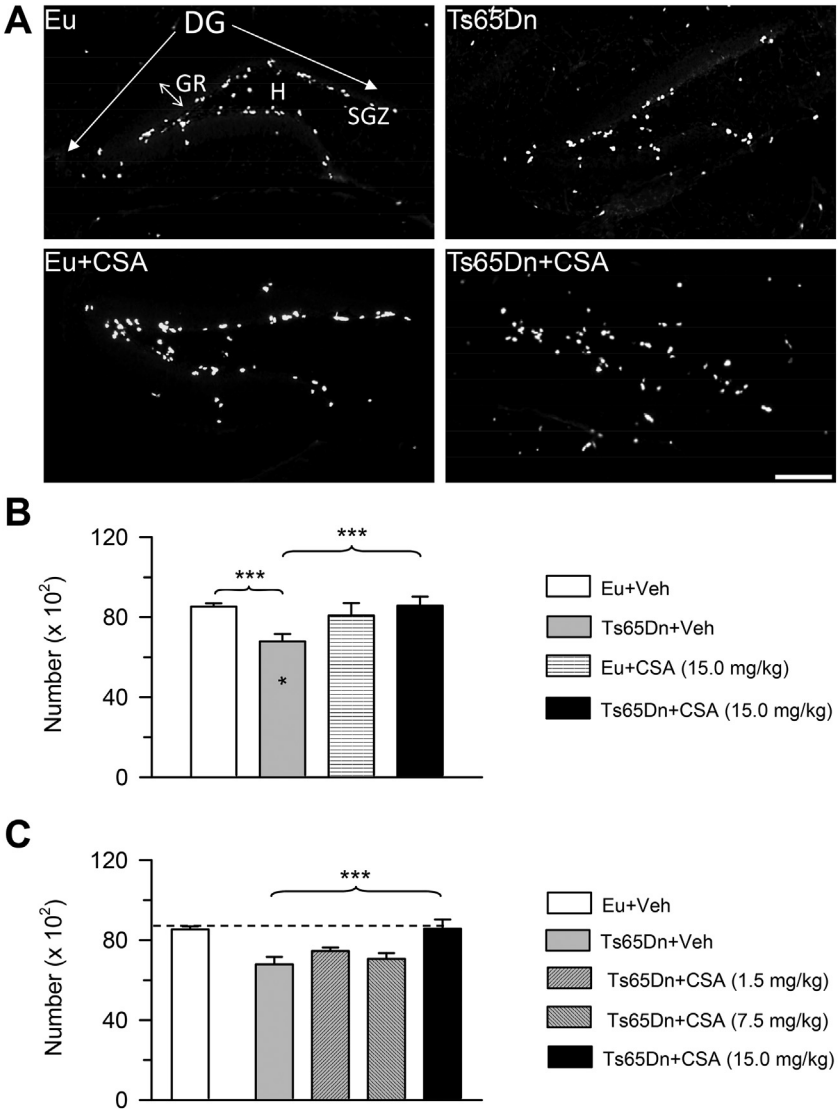

Fig. 2. Effects of neonatal treatment with CSA on the size of the population of cells in the S-phase of the cell cycle in the dentate gyrus of Ts65Dn and euploid mice.
A: Representative images of sections immunostained for BrdU from the dentate gyrus of untreated euploid and Ts65Dn mice, and of euploid and Ts65Dn mice that were treated daily with 15.0 mg/kg of CSA in the period P3-P15. Calibration bar = 200 μm. B: Total number of BrdU-positive cells in the dentate gyrus of untreated euploid (n = 5) and Ts65Dn (n = 6) mice, and of treated euploid (n = 4) and Ts65Dn (n = 5) mice.
C: Number of BrdU-positive cells in the dentate gyrus of Ts65Dn mice that received a daily injection of vehicle (n = 6; same mice as in B) or 1.5 mg/kg (n = 6), 7.5 mg/kg (n = 4), and 15.0 mg/kg (n = 5; same mice as in B) of CSA in the period P3-P15. The number of BrdU-positive cells in euploid mice that received the vehicle reported in (B) is shown for comparison. Values (mean ± SE) refer to one hemisphere. * $p \leq .05$; *** $p \leq .001$ (Fisher's LSD test after two-way ANOVA). Black asterisks in the gray bar indicate a difference between untreated Ts65Dn mice and treated euploid mice. Abbreviation: CSA, cyclosporine A; Eu, euploid; GR, granule cell layer; H, hilus; SGZ, subgranular zone; Veh, vehicle.

Kruskal-Wallis test showed a significant effect of treatment on granule cell density [χ^2 (3) = 12.149, $p < .007$]. The Mann-Whitney test showed a reduced granule cell density in Ts65Dn mice compared to euploid mice (U = 0.001, $p = .004$) and demonstrated that treatment caused an increase in granule cell density (U = 0.001, $p = .006$) (Fig. 4C). A two-way ANOVA on total number of granule cells showed no genotype x treatment interaction, but did demonstrate a main effect of genotype [F(1,17) = 19.301, $p = .001$], and of treatment [F (1,17) = 15.844, $p = .0.001$]. A *post hoc* Fisher's LSD test showed that untreated Ts65Dn mice had a reduced number of granule cells in comparison with euploid mice and that treatment restored granule cell number (Fig. 4D). A two-way ANOVA on the thickness of the granule cell layer showed no genotype x treatment interaction, whereas a main effect of genotype [F(1,16) = 4.742, $p = .045$] was present, as was a main effect of treatment [F(1,16) = 6.039, $p = .026$]. A *post hoc* Fisher's LSD test showed that the granule cell layer of untreated Ts65Dn mice had a reduced thickness in comparison with that of euploid mice and that this reduction was restored by treatment (Fig. 4E).

At variance with the neocortex, the granule cell layer develops according to an outside-inside pattern. Therefore, the older neurons occupy the superficial part of the granule cell layer and the younger neurons occupy its lower portion. In Hoechst-stained sections, the younger neurons are recognizable due to their smaller size and a more translucent pattern in comparison with the older neurons (Fig. 4A). We deemed it of interest to evaluate the thickness of the region of the granule cell layer that was occupied by younger neurons (see the double-headed black arrow in Fig. 4A). A two-way ANOVA on the thickness of the inner granule cell layer showed a genotype x treatment interaction [F(1,17) = 7.477, $p = .014$] and a main effect of genotype [F(1,17) =0.5.791, $p = .028$], but no main effect of treatment. Fisher's LSD test, carried out *post hoc*, showed that the inner part of the granule cell layer of untreated Ts65Dn mice was reduced in thickness compared to that of euploid mice and that this reduction was restored by treatment (Fig. 4F). The expansion of the inner part of the granule cell layer in treated Ts65Dn mice indicates that the treatment-induced increase in the proliferation rate of granule cells precursors in the SGZ of Ts65Dn mice (see above) translates into an increase in the number of new granule neurons that are added to the inner part of the granule cell layer and, hence, in total granule cell number. Unlike in Ts65Dn mice, in euploid mice drug treatment had no effect on the stereology of the granule cell layer (Fig. 4B-F), which is consistent with the absence of effects on the proliferation rate of the granule cell precursors.

5.4. *Effect of CSA on dendritic spine density in the dentate gyrus of Ts65Dn mice*

Spine density reduction is a typical feature of the trisomic brain (Benavides-Piccione et al., 2004; Guidi et al., 2013) that, in conjunction

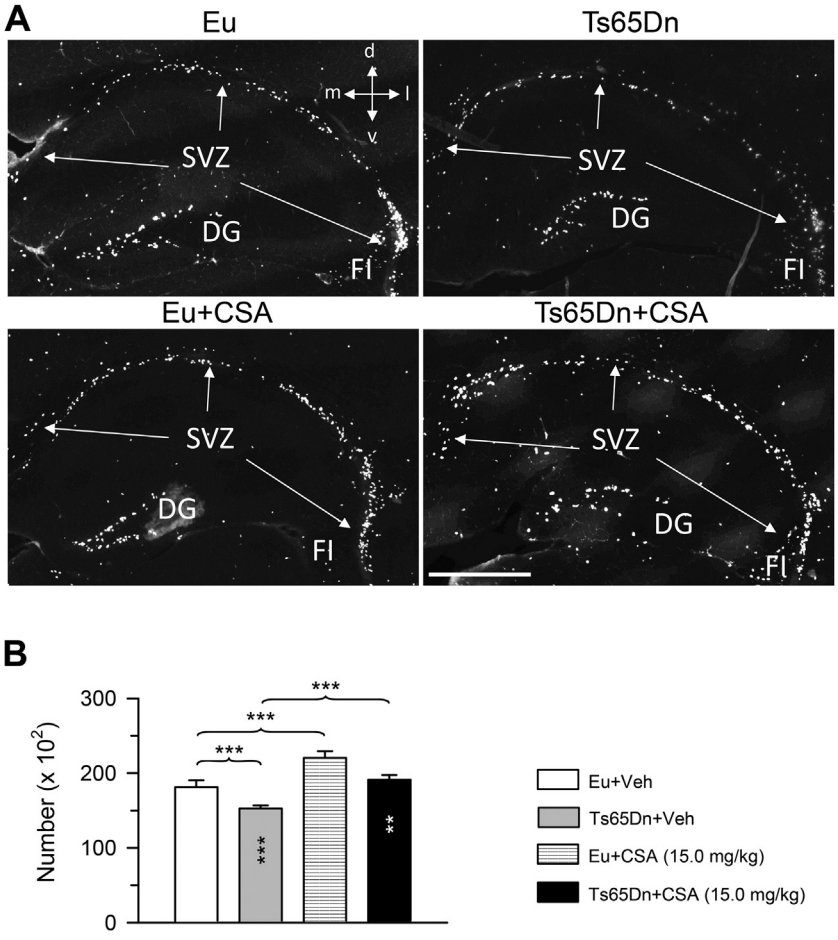

Fig. 3. Effects of neonatal treatment with CSA on the size of the population of cells in the S-phase of the cell cycle in the SVZ zone of Ts65Dn and euploid mice.
A: Representative images of sections immunostained for BrdU from the SVZ of untreated euploid and Ts65Dn mice, and of euploid and Ts65Dn mice that were treated daily with CSA in the period P3-P15. Calibration bar = 500 μm. B: Total number of BrdU-positive cells in the SVZ of untreated euploid (n = 5) and Ts65Dn (n = 6) mice, and of euploid (n = 4) and Ts65Dn (n = 5) mice treated with CSA. Values (mean ± SE) refer to one hemisphere. ** p ≤ .01; *** p ≤ .001 (Fisher's LSD test after two-way ANOVA). Black asterisks in the gray bar indicate a difference between untreated Ts65Dn mice and treated euploid mice. White asterisks in the black bar indicate a difference between treated Ts65Dn mice and treated euploid mice. Abbreviations: CSA, cyclosporine A; d, dorsal; Eu, euploid; DG, dentate gyrus; FI, fimbria; l, lateral; m, medial; SVZ, subventricular zone; v, ventral; Veh, vehicle.

with hypocellularity, is thought to be a critical determinant of intellectual disability. In order to establish whether CSA improves spine density, in Golgi-stained brains we evaluated spine density in the dendritic arbor of the granule neurons. Since the inputs to the dendritic tree of granule cells are organized in a laminar manner, we deemed it of interest to separately evaluate spine density in dendritic branches harbored in the outer half and inner half of the molecular layer. The examples of Golgi-stained dendritic branches reported in Fig. 5A clearly show that treatment causes a patent increase in spine density both in euploid and Ts65Dn mice. A two-way ANOVA on spine density in the proximal dendrites showed a genotype x treatment interaction [$F(1,17) = 20.174$, $p = .001$], a main effect of genotype [$F(1,17) = 6.803$, $p = .018$], and a main effect of treatment [$F(1,17) = 180.800$, $p < .001$]. A *post hoc* Fisher's LSD test showed that the spine density of untreated Ts65Dn mice was significantly reduced (−24%) in comparison with that of untreated euploid mice (Fig. 5B,C). After treatment with CSA the number of spines of Ts65Dn mice underwent a notable increment (+78% *vs.* untreated Ts65Dn mice) and became larger (+36%) than that of untreated euploid mice (Fig. 5B,C). A large increase in spine density (+30%) also took place in treated euploid mice (Fig. 5B,C). A two-way ANOVA on spine density in the distal dendrites showed a genotype x treatment interaction [$F(1,17) = 18.574$, $p = .001$], a main effect of genotype [$F(1,17) = 4.748$, $p = .044$], and a main effect of treatment [$F(1,17) = 136.054$, $p < .001$]. A *post hoc* Fisher's LSD test showed a significantly reduced spine density (−21%) in untreated Ts65Dn mice compared to untreated euploid mice (Fig. 5B,C). After treatment with CSA the number of spines of Ts65Dn mice underwent a notable increment (+64% *vs.* untreated Ts65Dn mice) and became larger (+30%) than that of euploid mice (Fig. 5B,C). A large increase in spine density (+23%) also took place in treated euploid mice (Fig. 5B,C).

5.5. Effect of CSA on p21 levels in the hippocampal formation of Ts65Dn mice

Elongation of the cell cycle and a precocious exit from the cell cycle appear to be key mechanisms underlying the typical impairment of neurogenesis that characterizes DS. Overexpression of p21 in the trisomic brain appears to be an important determinant involved in cell cycle alteration and, hence, in the reduction in proliferation rate (see (Stagni et al., 2018)). A two-way ANOVA on the p21 levels in the hippocampal formation showed no genotype x treatment interaction, and no main effect of genotype or of treatment. A *post hoc* Fisher's LSD test showed that untreated Ts65Dn mice had higher levels of p21 in comparison with euploid mice and that treatment with CSA reduced p21 levels to an extent that they became similar to those of euploid mice (Fig. 6B). In euploid mice, treatment had no effect on p21 levels (Fig. 6B).

5.6. General effects of CSA

The Ts65Dn strain is characterized by a high mortality rate during gestation and before weaning (Roper et al., 2006). The total number of mice used in the *in vivo* study was 81 (vehicle-treated mice: $n = 42$; CSA-treated mice $n = 39$). Three vehicle-treated (7.1%) and three CSA-treated (7.7%) mice died in the P3-P15 period. The similarity in the mortality rate across groups suggests that treatment has no adverse effects on the health of mice. We evaluated the body and brain weight of P15 mice that received vehicle or CSA (15.0 mg/kg) in order to establish the outcome of treatment on growth. A two-way ANOVA on

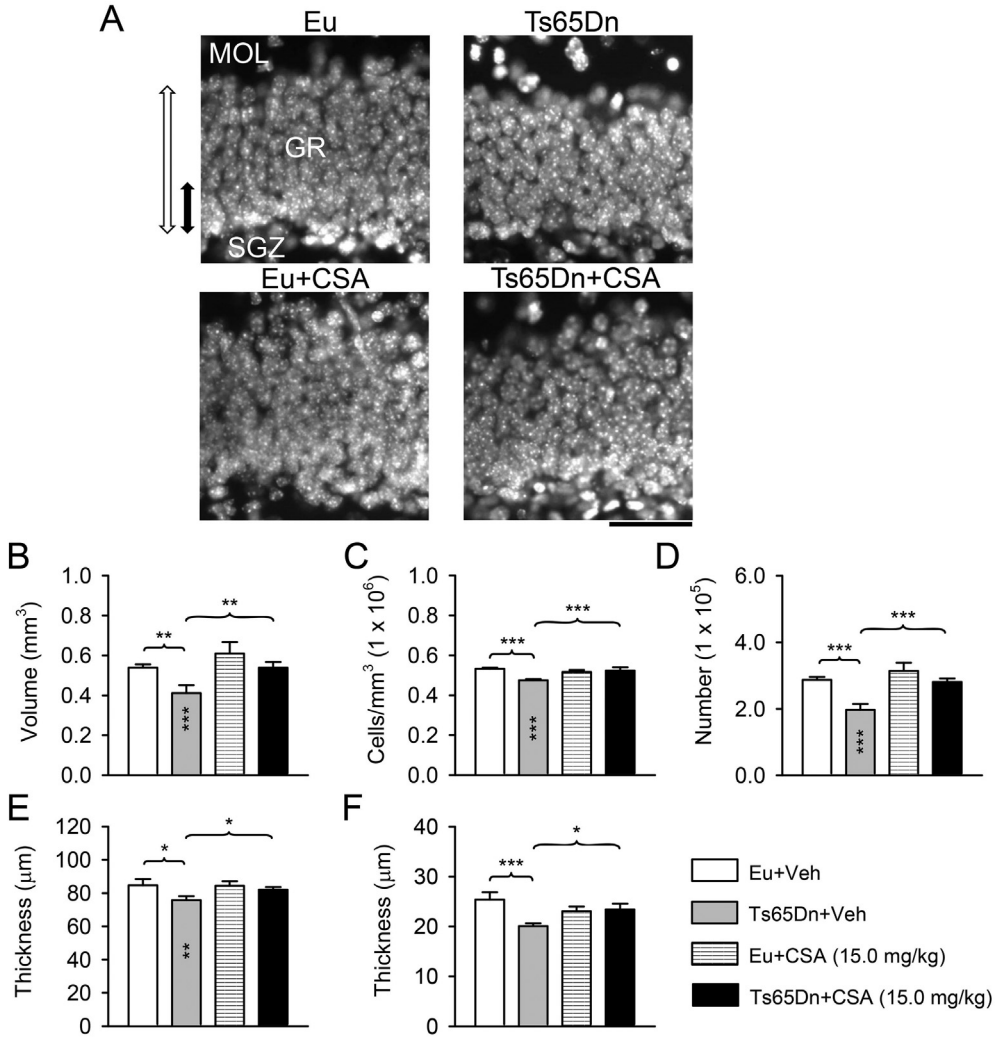

Fig. 4. Effects of neonatal treatment with CSA on the stereology of the granule cell layer of Ts65Dn and euploid mice.
A: Representative images of Hoechst-stained sections showing the granule cell layer of an animal from each experimental group. The double-headed white arrow indicates the thickness of the granule cell layer, while the double-headed black arrow indicates the thickness of the innermost part of the granule cell layer. Calibration bar = 50 µm. B-F: Volume of the granule cell layer (B), granule cell density (C), total number of granule cells (D), thickness of the granule cell layer (E), and thickness of the innermost part of the granule cell layer (F) of untreated euploid (n = 6) and Ts65Dn (n = 6) mice, and of euploid (n = 4) and Ts65Dn mice (n = 5) treated with CSA. Values (mean ± SE) refer to one dentate gyrus. * $p \leq .05$; ** $p \leq .01$; *** $p \leq .001$ (Fisher's LSD test after two-way ANOVA for data reported in B and D-F; Mann-Whitney test after Kruskal-Wallis test for data reported in C). Black asterisks in the gray bar indicate a difference between untreated Ts65Dn mice and treated euploid mice. Abbreviations: CSA, cyclosporine A; Eu, euploid; GR, granule cell layer; MOL, molecular layer; SGZ, subgranular zone; Veh, vehicle.

body weight showed a genotype x treatment interaction [$F(1,64) = 6.826$, $p = .011$] and a main effect of genotype [$F(1,64) = 29.560$, $p < .001$], but no main effect of treatment. A *post hoc* Fisher's LSD test showed that untreated and treated Ts65Dn mice had a lower body weight compared to their euploid counterparts (Table 1). A comparison of the body weight of treated and untreated mice showed that treated Ts65Dn mice had a similar body weight in comparison with their untreated counterparts and that treated euploid mice had a larger body weight in comparison with their untreated counterparts (Table 1). These findings indicate that treatment has no adverse effects on somatic growth. A two-way ANOVA on brain weight showed no genotype x treatment interaction, while a main effect of genotype [$F(1,64) = 14.117$, $p < .001$] and a main effect of treatment [$F(1,64) = 7.899$, $p = .007$] were present. A *post hoc* Fisher's LSD test showed that untreated and treated Ts65Dn mice had a lower brain weight compared to their euploid counterparts (Table 1). A comparison of the brain weight of treated and untreated mice showed that treated euploid and Ts65Dn mice had a reduced brain weight in comparison with their untreated counterparts (Table 1). Observation of the values reported in Table 1 shows that the brain weight reduction was 4% in treated *vs.* untreated euploid mice and 5% in treated *vs.* untreated Ts65Dn mice. This evidence shows that treatment exerts a moderately negative effect on brain growth.

6. Discussion

6.1. CSA positively impacts on proliferation, differentiation and maturation of trisomic NPCs

By exploiting cultures of NPCs from the SVZ, we found that CSA i) restores the reduced proliferation rate that characterizes trisomic NPCs; ii) increases the number of cells that differentiate into neurons and, concomitantly, reduces the number of cells that differentiate into astrocytes; iii) fosters development of neuritic processes; iv) does not affect cell death. The pro-proliferative and pro-neuronogenic effects of CSA found here in trisomic NPCs are consistent with evidence obtained in neurospheres from the dentate gyrus of wild type mice, showing that CSA increases both the number of neurospheres and the frequency of neuron-containing neurospheres relative to those containing glia (Chow and Morshead, 2016) at the same concentrations as those used here. It has been shown that CSA increases neurite outgrowth of cultured dorsal root ganglion cells with an EC_{50} of 50 nM (see (Hamilton and Steiner, 1998)). This is in line with the current findings that CSA fosters neurite outgrowth of trisomic NPCs and that concentrations as low as 3 nM are sufficient to elicit this effect.

6.2. Neonatal treatment with CSA restores neurogenesis and spinogenesis in the Ts65Dn mouse

In view of potential pharmacotherapies for DS, it is of obvious importance to demonstrate that the effects observed *in vitro* also take place

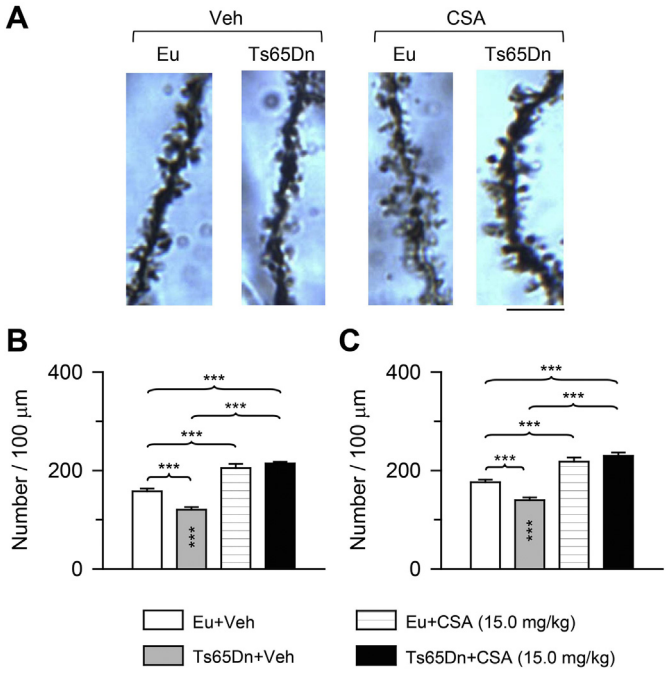

Fig. 5. Effects of neonatal treatment with CSA on dendritic spine density in the dentate gyrus of Ts65Dn and euploid mice.
A: Photomicrographs of Golgi-stained granule cell dendrites showing spines on distal dendritic branches in an animal from each experimental group. Calibration bar = 5 µm. B,C: Spine density on dendritic branches in the inner (B) and outer (C) half of the dendritic tree of the granule cells of untreated euploid (n = 6) and Ts65Dn mice (n = 6) and euploid (n = 4) and Ts65Dn (n = 5) mice treated with CSA. Values in (B,C) are mean ± SE. *** $p \leq .001$ (Fisher's LSD test after two-way ANOVA). Black asterisks in the gray bar indicate a difference between untreated Ts65Dn mice and treated euploid mice. Abbreviations: CSA, cyclosporine A; Eu, euploid; Veh, Vehicle.

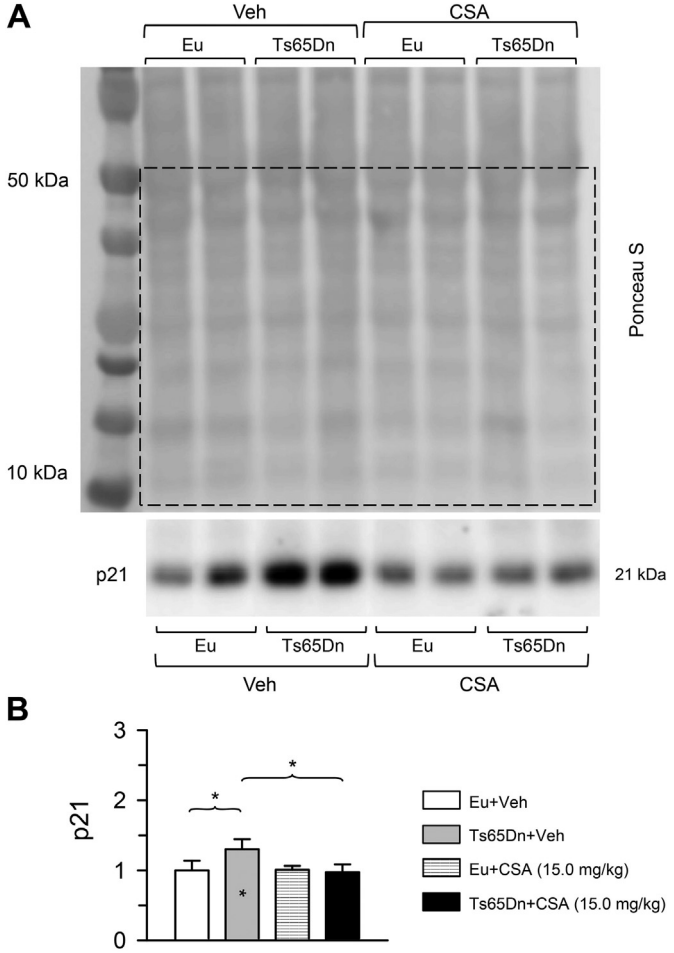

Fig. 6. Effects of neonatal treatment with CSA on p21 protein levels in the hippocampal formation of Ts65Dn and euploid mice.
A: Representative western blot showing immunoreactivity for p21 and Ponceau S-stained gel. Protein levels of p21 were normalized to all proteins with molecular weight between 10 and 50 kDa, as indicated by the dashed rectangle. B: Levels of p21 were examined in untreated euploid mice (n = 11), untreated Ts65Dn mice (n = 12), treated euploid mice (n = 10), and treated Ts65Dn mice (n = 8). One untreated euploid mouse (yielding 10) and one untreated Ts65Dn mouse (yielding 11) were excluded from p21 analysis. Protein levels (mean ± SE) are expressed as fold difference in comparison with untreated euploid mice. * $p \leq .05$ (Fisher's LSD test after two-way ANOVA). Black asterisks in the gray bar indicate a difference between untreated Ts65Dn mice and treated euploid mice. Abbreviations: CSA, cyclosporine A; Eu, euploid; Veh, vehicle.

in the greater complexity of the *in vivo* condition. Our results show that in Ts65Dn pups treated with CSA for 13 days there was full restoration of the number of BrdU-positive cells in the dentate gyrus and SVZ, indicating that treatment positively impacts on the two major forebrain neurogenic niches. An evaluation of the pro-neurogenic effects of three different doses of CSA showed that a dose of 15 mg/kg/day (but not lower doses) was able to fully rescue cell proliferation in Ts65Dn mice. It is worthy to note, that the 15.0 mg/kg dose translates into approximately 1.2 mg/kg/day in the human setting (Reagan-Shaw et al., 2008). The finding that the lower doses tested here did not increase NPC proliferation suggests a threshold for the pro-neurogenic effects of CSA.

The NPCs of the SGZ give origin to granule neurons and astrocytes destined to the dentate gyrus. In agreement with the pro-*neuronogenic* effect observed *in vitro*, in treated Ts65Dn mice there was an increase in the size of the innermost part of the granule cell layer, which harbors the newly-generated granule cells. This effect was accompanied by a large increase in the volume and thickness of the granule cell layer and total number of granule cells. The NPCs of the SVZ give origin to granule cells destined to the olfactory bulb and to astrocytes and oligodendrocytes destined to the cortex (Brazel et al., 2003). This suggests that the CSA-induced increase in the proliferation potency of NPCs in the SVZ may positively impact on postnatal development of the olfactory bulb and neocortex.

In the current study, we were interested in establishing whether treatment with CSA can ameliorate the severe spine density reduction that characterizes the granule cells of the dentate gyrus of Ts65Dn mice. We found that CSA largely enhanced the process of spinogenesis and that Ts65Dn mice treated with CSA underwent a large increase in spine density that even surpassed that of euploid mice. The effect took place along the whole extent of the dendritic tree of the granule cells. The major extrinsic input to the hippocampal formation is constituted by the perforant pathway, which takes its origin from the medial and lateral divisions of the entorhinal cortex (Amaral and Witter, 1995). Both inputs are fundamental for the participation of the hippocampal formation in long-term memory functions. The medial perforant pathway terminates on the middle third of the dendritic tree of the granule cells, while the lateral perforant pathway terminates on the outer third. The treatment-induced increase in spine density on proximal and distal dendrites suggests that this effect may lead to restoration of the memory functions mediated by both divisions of the entorhinal cortex.

There are several candidates for the molecular mechanisms underlying NPC proliferation impairment in DS, among which p21 may be a particularly critical one. The protein p21, also known as cyclin-dependent kinase inhibitor 1 or CDK-interacting protein 1, is overexpressed in the brain of fetuses with DS and in the Ts65Dn model (Engidawork et al., 2001; Stagni et al., 2015). Since p21 inhibits the

transition from the G1 to the S-phase of the cell cycle, its overexpression may be a key determinant of proliferation impairment in DS. We found here that treatment with CSA normalized the levels of p21 in the hippocampal formation of Ts65Dn mice, suggesting that this effect may underlie restoration of proliferation. CSA is classically known to inhibit in T-lymphocytes the activity of the calcineurin-NFAT pathway and this effect is mediated by its binding to cyclophilin A. For this reason, it is used in a clinical setting in order to prevent graft rejection in organ transplantation. CSA, however, has a high affinity for other cyclophilins (B, C, D) (Hamilton and Steiner, 1998) and can therefore modulate various signaling pathways and exert calcineurin-independent effects (Sachewsky et al., 2014). It is worth noting that CSA appears to block the activity of the p38 signaling pathway (Matsuda and Koyasu, 2000), one of the three subgroups of the mitogen-activated protein kinase superfamily. Activation of p38 increases the mRNA and protein levels of the transcription factor p53 which, in turn, promotes the transcription of various genes, including p21 (Saha et al., 2014). In the brain of individuals with DS there is an increased activation of p38 and p53 (Swatton et al., 2004; Tramutola et al., 2016), and increased activation of p53 has also been detected in the brain of the Ts65Dn model (Tramutola et al., 2016). Thus, the inhibitory effect exerted by CSA on the p38 pathway may account for the normalization of p21 levels found here in treated Ts65Dn mice and, hence, restoration of proliferation.

Several protein kinases, including p38, are essential factors in spine growth (Tada and Sheng, 2006). It has been shown that inhibition of p38 activity increases the size and number of dendritic spines (Fernandez et al., 2012) and that in p38 heterozygous knockdown mice there is an increase in dendritic spine density (Dai et al., 2016). In view of the inhibitory role of p38 in spine morphogenesis, it seems reasonable to hypothesize that the spine density increase observed here in CSA-treated mice may be attributable to a CSA-mediated inhibition of p38.

6.3. Conclusions and future perspectives

DS is characterized by impairment of NPC proliferation, acquisition of a neuronal phenotype, and dendritic development. An obvious question regards the possibility of pharmacologically restoring this whole triad of defects. While the gene burden is the *primum movens* of overall brain and somatic alterations in DS, it is likely that the triad of DS neurodevelopmental defects is attributable to the alteration of specific pathways. In view of the complexity of these alterations, it may be necessary to use drug combinations in order to fully correct brain development. Importantly, the current study shows that treatment with a single drug, CSA, administered for a short but critical time window, is able to restore the entire triad of defects of the trisomic brain.

In view of its extensive effects in the murine model, CSA may be potentially effective in DS patients. However, caution must be exercised because CSA is an immunosuppressant and its clinical use is limited by side effects that include nephrotoxicity, neurotoxicity and hepatotoxicity (Matsuda and Koyasu, 2000; Bartynski et al., 2001). A recent study shows that three children with DS treated with CSA (approximately 6 mg/kg/day) as therapy for idiopathic aplastic anemia did not experience severe or unexpected adverse events during treatment (Suzuki et al., 2016). Another report describes the case of a girl with DS treated with prednisone and CSA (about 4 mg/kg twice a day) for the treatment of alopecia. This report does not describe adverse effects of treatment either (Gensure, 2013). In both studies, the treatment lasted for months. Although these studies show that CSA is a tolerated treatment in individuals with DS, the possibility of side effects must be taken into account. To this regard, it is noteworthy that we did not observe apparent effects of 13 day-long CSA treatment on mice health status, as evidenced by no change in body weight of both genotypes. Conversely, in treated mice we found a small (4–5%) reduction in overall brain weight, which is in line with similar evidence obtained in rats (Setkowicz and Kadulski, 2007). The causes of this brain weight reduction remain to be elucidated. Recent evidence shows that brain protein turnover is much higher than previously assumed (3–4% day) which makes the brain prone to undergo considerable remodeling (Smeets et al., 2018). It has been shown that CSA inhibits protein synthesis in rat liver (Backman et al., 1988). If a similar effect takes place in the brain, this may explain the brain weight reduction found here in CSA-treated mice. There is evidence that while CSA does not change the overall density of Nissl-stained neurons in rats, it reduces the number of calretinin-and parvalbumin-positive neurons (Setkowicz and Kadulski, 2007), the number of glioma-infiltrating microglial cells (Gabrusiewicz et al., 2011), and the survival of reactive astrocytes in culture (Pyrzynska et al., 2001). It cannot be ruled out that the brain weight reduction observed here after treatment with CSA may be due to a reduction in the number of some cells populating the brain. An important issue that needs to be addressed in further studies will be to establish whether a shorter treatment schedule can restore the neurodevelopmental defects of DS without affecting overall brain weight.

The toxicity of CSA appears to be largely tied to its calcineurin-mediated mechanism of action. It must be remarked that various studies have shown that the immunosuppressive and neurotrophic actions of immunosuppressants can be dissociated and that the neurotrophic properties of immunosuppressant drugs are not mechanistically linked to their immunosuppressive actions but operate by separate pathways (see (Hamilton and Steiner, 1998, Nigro et al., 2013)). Non-immunosuppressant analogues of CSA (and of other immunosuppressant drugs such as FK506) have been shown to bind to their respective immunophilins and inhibit their activity, but they lack the ability to interact with calcineurin. For instance, a non-immunosuppressive analogue of CSA (MeAla-6-CsA) stimulates neurite outgrowth of PC12 cells, similarly to the action of CSA (Steiner et al., 1997), and the non-immunosuppressive analogue of CSA NIM811 mimics the pro-survival effects of CSA on NPCs *in vitro* (Sachewsky et al., 2014). The immunosuppressive effect of CSA may represent a serious liability in the context of treatment for DS. However, by exploiting non-immunosuppressive analogues of CSA it may be possible to obtain the same positive effects on brain development as those elicited by CSA, in absence of unwanted effects due to immunosuppression. We hope that our study may prompt further work to clarify this important issue. If CSA analogues prove to have the same positive impact as CSA on neurogenesis and spinogenesis they may be considered as practicable tools for ameliorating brain development in individuals with DS.

Supplementary data to this article can be found online at https://doi.org/10.1016/j.nbd.2019.05.005.

Acknowledgment

This work was supported by grants to R. B. from “Fondazione Generali e Assicurazione Generali” (GENERALIBA2017), Italy, and “Fondazione del Monte” (DELMONBART2014), Italy. The assistance of Melissa Stott in the revision of the language and the technical assistance of Mr. Francesco Campisi and Mr. Massimo Verdosci are gratefully acknowledged.

Conflict of interest

The authors declare that they have no conflict of interest.

References

Altman, J., Bayer, S., 1975. Postnatal development of the hippocampal dentate gyrus under normal and experimental conditions. In: Isaacson, R.L., Pribram, K.H. (Eds.), The Hippocampus. vol. 1. Plenum Press, New York and London, pp. 95–122.

Amaral, D.G., Witter, M.P., 1995. Hippocampal formation. In: Paxinos, G. (Ed.), The Rat Nervous System. Academic Press, pp. 443–492.

Backman, L., Appelkvist, E.L., Dallner, G., 1988. Influence of cyclosporine A on protein synthesis in rat liver. Exp. Mol. Pathol. 49, 38–49.

Bartynski, W.S., Zeigler, Z., Spearman, M.P., Lin, L., Shadduck, R.K., Lister, J., 2001.

Etiology of cortical and white matter lesions in cyclosporin-A and FK-506 neurotoxicity. AJNR Am. J. Neuroradiol. 22, 1901–1914.
Benavides-Piccione, R., Ballesteros-Yanez, I., de Lagran, M.M., Elston, G., Estivill, X., Fillat, C., Defelipe, J., Dierssen, M., 2004. On dendrites in Down syndrome and DS murine models: a spiny way to learn. Prog. Neurobiol. 74, 111–126.
Bianchi, P., Ciani, E., Contestabile, A., Guidi, S., Bartesaghi, R., 2010a. Lithium restores neurogenesis in the subventricular zone of the Ts65Dn mouse, a model for down syndrome. Brain Pathol. 20, 106–118.
Bianchi, P., Ciani, E., Guidi, S., Trazzi, S., Felice, D., Grossi, G., Fernandez, M., Giuliani, A., Calza, L., Bartesaghi, R., 2010b. Early pharmacotherapy restores neurogenesis and cognitive performance in the Ts65Dn mouse model for Down syndrome. J. Neurosci. 30, 8769–8779.
Brazel, C.Y., Romanko, M.J., Rothstein, R.P., Levison, S.W., 2003. Roles of the mammalian subventricular zone in brain development. Prog. Neurobiol. 69, 49–69.
Chow, A., Morshead, C.M., 2016. Cyclosporin A enhances neurogenesis in the dentate gyrus of the hippocampus. Stem Cell Res. 16, 79–87.
Contestabile, A., Fila, T., Ceccarelli, C., Bonasoni, P., Bonapace, L., Santini, D., Bartesaghi, R., Ciani, E., 2007. Cell cycle alteration and decreased cell proliferation in the hippocampal dentate gyrus and in the neocortical germinal matrix of fetuses with Down syndrome and in Ts65Dn mice. Hippocampus 17, 665–678.
Contestabile, A., Greco, B., Ghezzi, D., Tucci, V., Benfenati, F., Gasparini, L., 2013. Lithium rescues synaptic plasticity and memory in Down syndrome mice. J. Clin. Invest. 123, 348–361.
Cvijetic, S., Bortolotto, V., Manfredi, M., Ranzato, E., Marengo, E., Salem, R., Canonico, P.L., Grilli, M., 2017. Cell autonomous and noncell-autonomous role of NF-kappaB p50 in astrocyte-mediated fate specification of adult neural progenitor cells. Glia 65, 169–181.
Dai, H.-L., Hu, W.-Y., Jiang, L.-H., Li, L., Gaung, X.-F., Xiao, Z.-C., 2016. p38 MAPK inhibition improves synaptic plasticity and memory in angiotensin II-dependent hypertensive mice. Sci. Rep. 6, 27600.
Dierssen, M., 2012. Down syndrome: the brain in trisomic mode. Nat. Rev. Neurosci. 13, 844–858.
Engidawork, E., Gulesserian, T., Seidl, R., Cairns, N., Lubec, G., 2001. Expression of apoptosis related proteins: RAIDD, ZIP kinase, Bim/BOD, p21, Bax, Bcl-2 and NF-kappaB in brains of patients with Down syndrome. J. Neural Transm. Suppl. 181–192.
Fernandez, F., Soon, I., Li, Z., Kuan, T.C., Min, D.H., Wong, E.S.-M., Demidov, O.N., Paterson, M.C., Dawe, G., Bulavin, D.V., Xiao, Z.-C., 2012. Wip1 phosphatase positively modulates dendritic spine morphology and memory processes through the p38MAPK signaling pathway. Cell Adhes. Migr. 6, 333–343.
Gabrusiewicz, K., Ellert-Miklaszewska, A., Lipko, M., Sielska, M., Frankowska, M., Kaminska, B., 2011. Characteristics of the alternative phenotype of microglia/macrophages and its modulation in experimental gliomas. PLoS One 6, e23902.
Gensure, R.C., 2013. Clinical response to combined therapy of cyclosporine and prednisone. J. Investig. Dermatol. Symp. Proc. 16, S58.
Giacomini, A., Stagni, F., Trazzi, S., Guidi, S., Emili, M., Brigham, E., Ciani, E., Bartesaghi, R., 2015. Inhibition of APP gamma-secretase restores Sonic Hedgehog signaling and neurogenesis in the Ts65Dn mouse model of Down syndrome. Neurobiol. Dis. 82, 385–396.
Guidi, S., Stagni, F., Bianchi, P., Ciani, E., Ragazzi, E., Trazzi, S., Grossi, G., Mangano, C., Calza, L., Bartesaghi, R., 2013. Early pharmacotherapy with fluoxetine rescues dendritic pathology in the Ts65Dn mouse model of Down syndrome. Brain Pathol. 23, 129–143.
Hamilton, G.S., Steiner, J.P., 1998. Immunophilins: beyond immunosuppression. J. Med. Chem. 41, 5119–5143.
Kempermann, G., Gage, F.H., 2002. Genetic influence on phenotypic differentiation in adult hippocampal neurogenesis. Brain Res. Dev. Brain Res. 134, 1–12.
Malberg, J.E., Eisch, A.J., Nestler, E.J., Duman, R.S., 2000. Chronic antidepressant treatment increases neurogenesis in adult rat hippocampus. J. Neurosci. 20, 9104–9110.
Matsuda, S., Koyasu, S., 2000. Mechanisms of action of cyclosporine. Immunopharmacology 47, 119–125.
Meneghini, V., Cuccurazzu, B., Bortolotto, V., Ramazzotti, V., Ubezio, F., Tzschentke, T.M., Canonico, P.L., Grilli, M., 2014. The noradrenergic component in tapentadol action counteracts mu-opioid receptor-mediated adverse effects on adult neurogenesis. Mol. Pharmacol. 85, 658–670.
Nigro, P., Pompilio, G., Capogrossi, M.C., 2013. Cyclophilin A: a key player for human disease. Cell Death Dis. 4, e888.
Pyrzynska, B., Lis, A., Mosieniak, G., Kaminska, B., 2001. Cyclosporin A-sensitive signaling pathway involving calcineurin regulates survival of reactive astrocytes. Neurochem. Int. 38, 409–415.
Reagan-Shaw, S., Nihal, M., Ahmad, N., 2008. Dose translation from animal to human studies revisited. FASEB J. 22, 659–661.
Reinholdt, L.G., Ding, Y., Gilbert, G.J., Czechanski, A., Solzak, J.P., Roper, R.J., Johnson, M.T., Donahue, L.R., Lutz, C., Davisson, M.T., 2011. Molecular characterization of the translocation breakpoints in the Down syndrome mouse model Ts65Dn. Mamm. Genome 22, 685–691.
Romero-Calvo, I., Ocon, B., Martinez-Moya, P., Suarez, M.D., Zarzuelo, A., Martinez-Augustin, O., de Medina, F.S., 2010. Reversible Ponceau staining as a loading control alternative to actin in Western blots. Anal. Biochem. 401, 318–320.
Roper, R.J., St John, H.K., Philip, J., Lawler, A., Reeves, R.H., 2006. Perinatal loss of Ts65Dn Down syndrome mice. Genetics 172, 437–443.
Sachewsky, N., Hunt, J., Cooke, M.J., Azimi, A., Zarin, T., Miu, C., Shoichet, M.S., Morshead, C.M., 2014. Cyclosporin A enhances neural precursor cell survival in mice through a calcineurin-independent pathway. Dis. Model. Mech. 7, 953–961.
Saha, K., Adhikary, G., Kanade, S.R., Rorke, E.A., Eckert, R.L., 2014. p38delta regulates p53 to control p21Cip1 expression in human epidermal keratinocytes. J. Biol. Chem. 289, 11443–11453.
Setkowicz, Z., Kadulski, J., 2007. Effects of Immunosuppressants FK506 and Cyclosporin A on the Developing Rat Brain.
Smeets, J.S.J., Horstman, A.M.H., Schijns, O.E.M.G., Dings, J.T.A., Hoogland, G., Gijsen, A.P., Goessens, J.P.B., Bouwman, F.G., Wodzig, W.K.W.H., Mariman, E.C., van Loon, L.J.C., 2018. Brain tissue plasticity: protein synthesis rates of the human brain. Brain 141, 1122–1129.
Stagni, F., Giacomini, A., Guidi, S., Ciani, E., Ragazzi, E., Filonzi, M., De Iasio, R., Rimondini, R., Bartesaghi, R., 2015. Long-term effects of neonatal treatment with fluoxetine on cognitive performance in Ts65Dn mice. Neurobiol. Dis. 74C, 204–218.
Stagni, F., Giacomini, A., Emili, M., Trazzi, S., Guidi, S., Sassi, M., Ciani, E., Rimondini, R., Bartesaghi, R., 2016. Short- and long-term effects of neonatal pharmacotherapy with epigallocatechin-3-gallate on hippocampal development in the Ts65Dn mouse model of Down syndrome. Neuroscience 333, 277–301.
Stagni, F., Giacomini, A., Guidi, S., Emili, M., Uguagliati, B., Salvalai, M.E., Bortolotto, V., Grilli, M., Rimondini, R., Bartesaghi, R., 2017. A flavonoid agonist of the TrkB receptor for BDNF improves hippocampal neurogenesis and hippocampus-dependent memory in the Ts65Dn mouse model of DS. Exp. Neurol. 298, 79–96.
Stagni, F., Giacomini, A., Emili, M., Guidi, S., Bartesaghi, R., 2018. Neurogenesis impairment: an early developmental defect in Down syndrome. Free Radic. Biol. Med. 114, 15–32.
Steiner, J.P., Connolly, M.A., Valentine, H.L., Hamilton, G.S., Dawson, T.M., Hester, L., Snyder, S.H., 1997. Neurotrophic actions of nonimmunosuppressive analogues of immunosuppressive drugs FK506, rapamycin and cyclosporin A. Nat. Med. 3, 421–428.
Suzuki, K., Muramatsu, H., Okuno, Y., Narita, A., Hama, A., Takahashi, Y., Yoshida, M., Horikoshi, Y., Watanabe, K.-I., Kudo, K., Kojima, S., 2016. Immunosuppressive therapy for patients with Down syndrome and idiopathic aplastic anemia. Int. J. Hematol. 104, 130–133.
Swatton, J.E., Sellers, L.A., Faull, R.L., Holland, A., Iritani, S., Bahn, S., 2004. Increased MAP kinase activity in Alzheimer's and Down syndrome but not in schizophrenia human brain. Eur. J. Neurosci. 19, 2711–2719.
Tada, T., Sheng, M., 2006. Molecular mechanisms of dendritic spine morphogenesis. Curr. Opin. Neurobiol. 16, 95–101.
Tozuka, Y., Fukuda, S., Namba, T., Seki, T., Hisatsune, T., 2005. GABAergic excitation promotes neuronal differentiation in adult hippocampal progenitor cells. Neuron 47, 803–815.
Tramutola, A., Pupo, G., Di Domenico, F., Barone, E., Arena, A., Lanzillotta, C., Brokeaart, D., Blarzino, C., Head, E., Butterfield, D.A., Perluigi, M., 2016. Activation of p53 in Down syndrome and in the Ts65Dn mouse brain is associated with a pro-apoptotic phenotype. J. Alzheimer's Dis. 52, 359–371.
Trazzi, S., Mitrugno, V.M., Valli, E., Fuchs, C., Rizzi, S., Guidi, S., Perini, G., Bartesaghi, R., Ciani, E., 2011. APP-dependent up-regulation of Ptch1 underlies proliferation impairment of neural precursors in Down syndrome. Hum. Mol. Genet. 20, 1560–1573.
Trazzi, S., Fuchs, C., Valli, E., Perini, G., Bartesaghi, R., Ciani, E., 2013. The amyloid precursor protein (APP) triplicated gene impairs neuronal precursor differentiation and neurite development through two different domains in the Ts65Dn mouse model for Down syndrome. J. Biol. Chem. 288, 20817–20829.
Trazzi, S., Fuchs, C., De Franceschi, M., Mitrugno, V., Bartesaghi, R., Ciani, E., 2014. APP-dependent alteration of GSK3ß activity impairs neurogenesis in the Ts65Dn mouse model of Down syndrome. Neurobiol. Dis. https://doi.org/10.1016/j.nbd.2014.03.003. (Epub ahead of print).